Supporting Information

Waterborne Dispersion-Processed Self-Healing Elastomers with Hydrogen-Bond Locked Hydrophobic Microdomains for Multifunctional Applications

Qianshu Wang,[1,2] Wenbo Luan,[1,2] Xiaodong Sui,[1,2] Qi Sun,[1,2] Mengyu Zhang,[1,2] Longhai Guo,[1,2] Jun Ye,[*1,2] Teng Qiu[*1,2] & Xinlin Tuo[*3]

1 Key Laboratory of Carbon Fiber and Functional Polymers, Ministry of Education, Beijing University of Chemical Technology, Beijing 100029, P.R. China

2 Beijing Engineering Research Center of Synthesis and Application of Waterborne Polymer, Beijing University of Chemical Technology, Beijing 100029, P.R. China

3 Key Laboratory of Advanced Materials (MOE), Department of Chemical Engineering, Tsinghua University, Beijing 100084, P. R. China

[*] Corresponding authors:

Ye Jun (yejun@mail.buct.edu.cn)

Teng Qiu (qiuteng@mail.buct.edu.cn)

Xinlin Tuo (tuoxl@mail.tsinghua.edu.cn)

Contents

Supplementary Tables and Figures

1 Experimental

Tab.S1 Synthesis Formulation of W-P-DA_2-*x*%

x%	$n_{(P\text{-}DA_2)}/n_{(IPDI)}$	PTMG(g)	IPDA(g)	DMBA(g)	BDO(g)	P-DA_2(g)	TEA(g)
0	\	20.00	8.89	1.63	0.88	\	1.11
1	4.10E-03	20.00	8.89	1.64	0.84	0.33	1.12
2	8.30E-03	20.00	8.89	1.66	0.79	0.66	1.13
3	1.26E-02	20.00	8.89	1.67	0.75	1.00	1.14
4	1.70E-02	20.00	8.89	1.69	0.70	1.35	1.15
5	2.14E-02	20.00	8.89	1.71	0.65	1.71	1.17

$R = n_{NCO} / (n_{OH} \bullet n_{NH2}) = 1.30$, which was controlled using a combination of P-DA_2 and BDO.

Tab.S2 Adhesion process parameters

Types	Coating area(cm^2)	Coating coverage rate($L\bullet m^{-2}$)	Pressure(MPa)	Temp(℃)	Time(min)
Al sheet	2.5×1.25	0.625	3.0	90	0.5
Cu sheet	2.5×1.25	0.625	0.5	90	0.5
Wood sheet	1.2×1.6	0.385	0.5	100	0.5
PE sheet	2.5×1.25	0.625	0.5	\	\
NBR	15×2.5	1.870	5.0	90	3.0
NR	15×2.5	1.870	5.0	90	3.0
PPTA	15×2.5	1.870	3.0	120	2.0

2 Synthesis of P-DA_2 and W-P-DA_2-x% dispersion

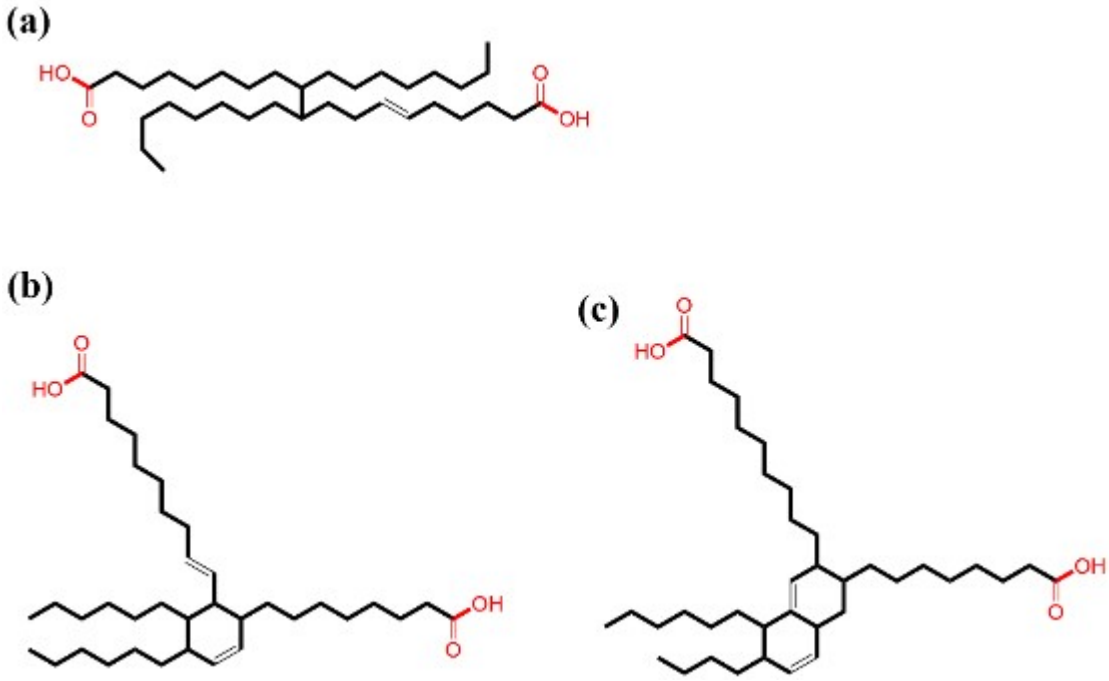

Fig.S1 Main chemical composition of DA.

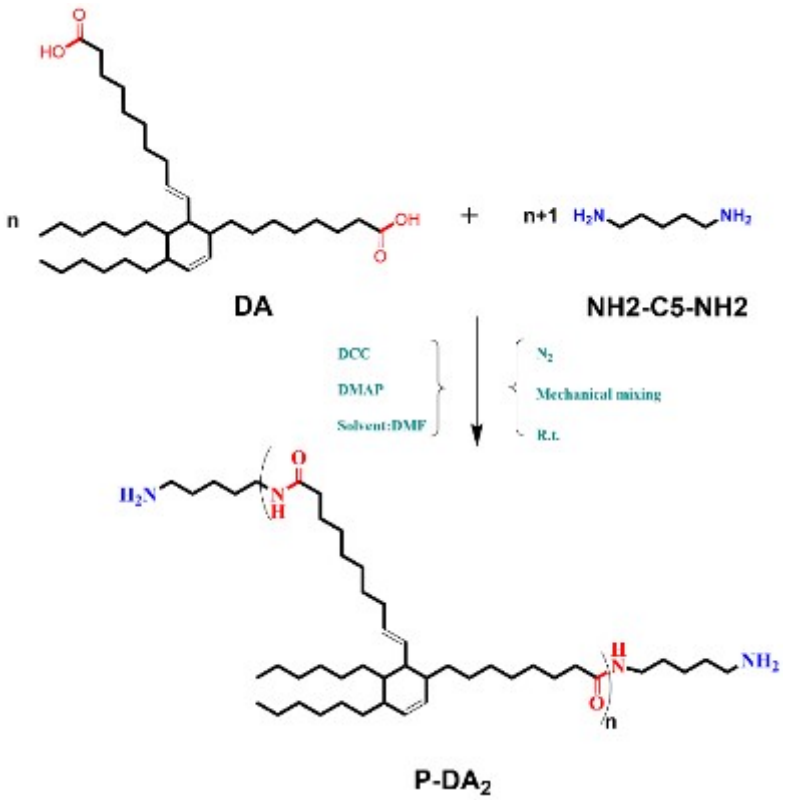

Fig.S2 Synthesis of P-DA_2.

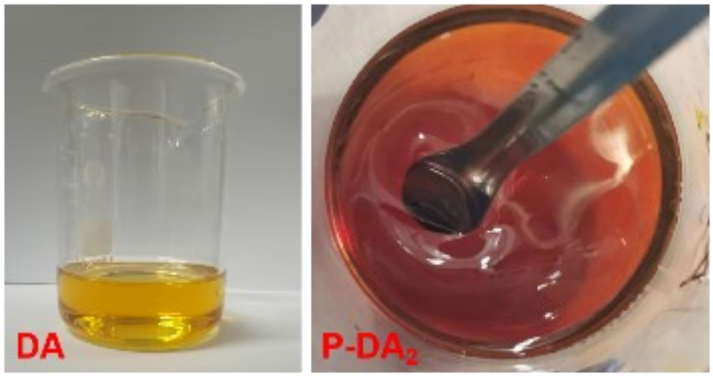

Fig.S3 Appearance of DA and P-DA_2 at room temperature.

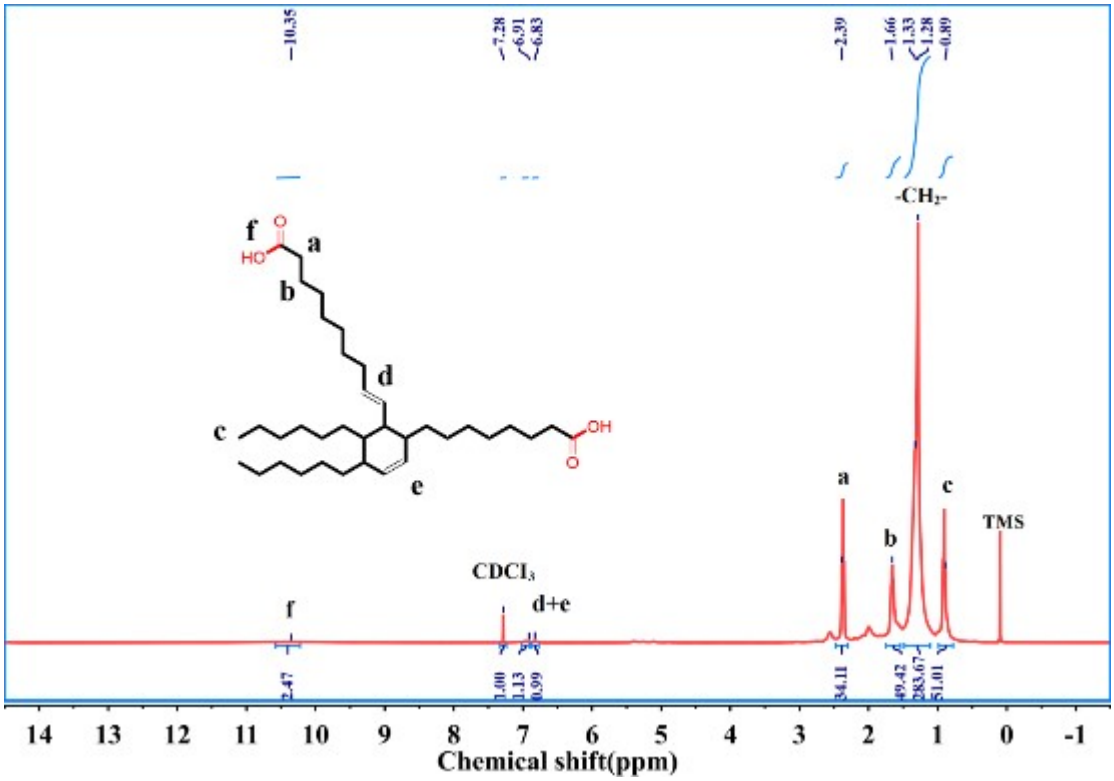

Fig.S4 ^{1}H NMR spectrum of DA.

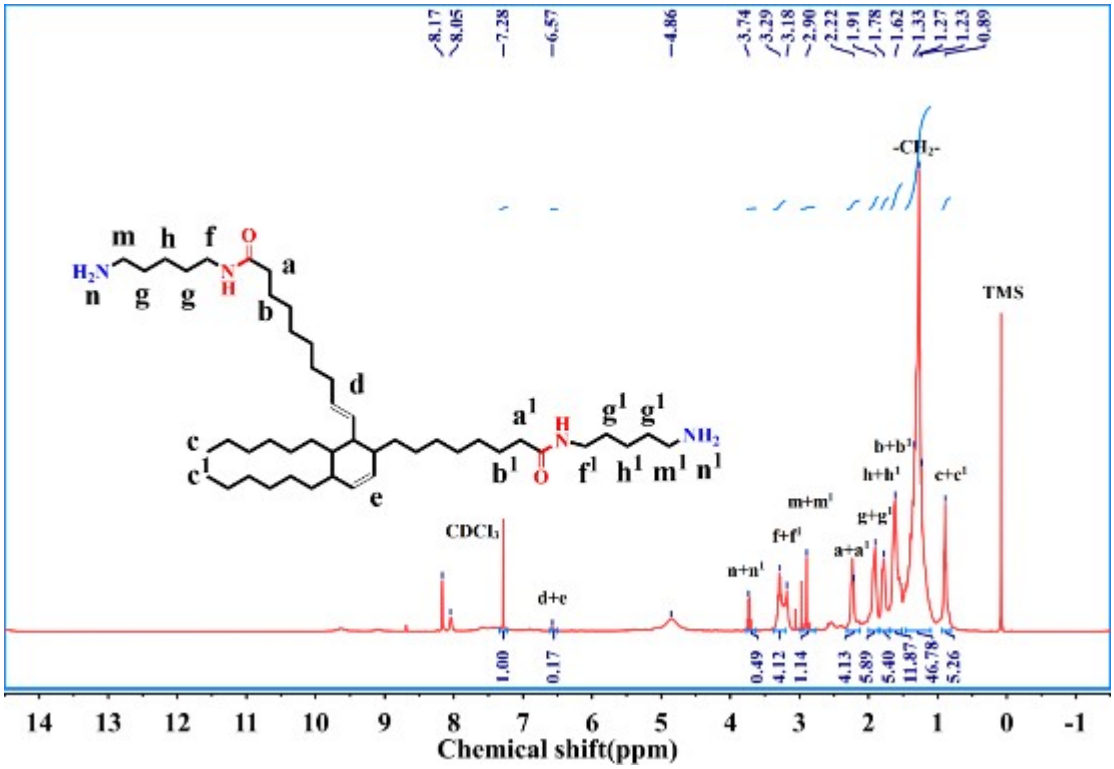

Fig.S5 ^{1}H NMR spectrum of P-DA$_2$.

The average degree of polymerization (n_1) is calculated by (Eq.S1) based on the

integral areas of the peak at 2.90 ppm ($I_{2.90}$, -CONH-CH_2-) and at 0.89 ppm ($I_{0.89}$, -CH_2CH_3), which is about 3.07.

$$n^1 = \frac{4\, I_{0.89,\ -CH_2CH_3}}{6\, I_{2.90,\ -CONH-CH_2}} \quad \text{.....(Eq.S1)}$$

Tab.S3 Molecular weight calculations by ^{1}H NMR.

$I_{2.90}$, -CONH-CH_2-	$I_{0.89}$, -CH_2CH_3	n^1	*Mn*
1.14	5.26	3.07	2.00×10^3 (2,159)

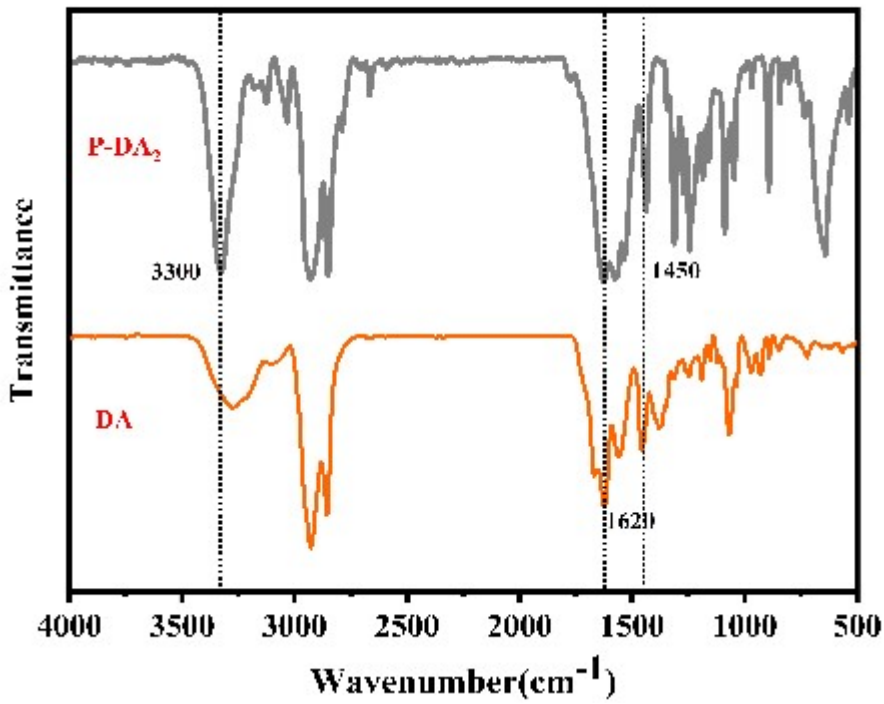

Fig.S6 FTIR spectra of DA and P-DA$_2$.

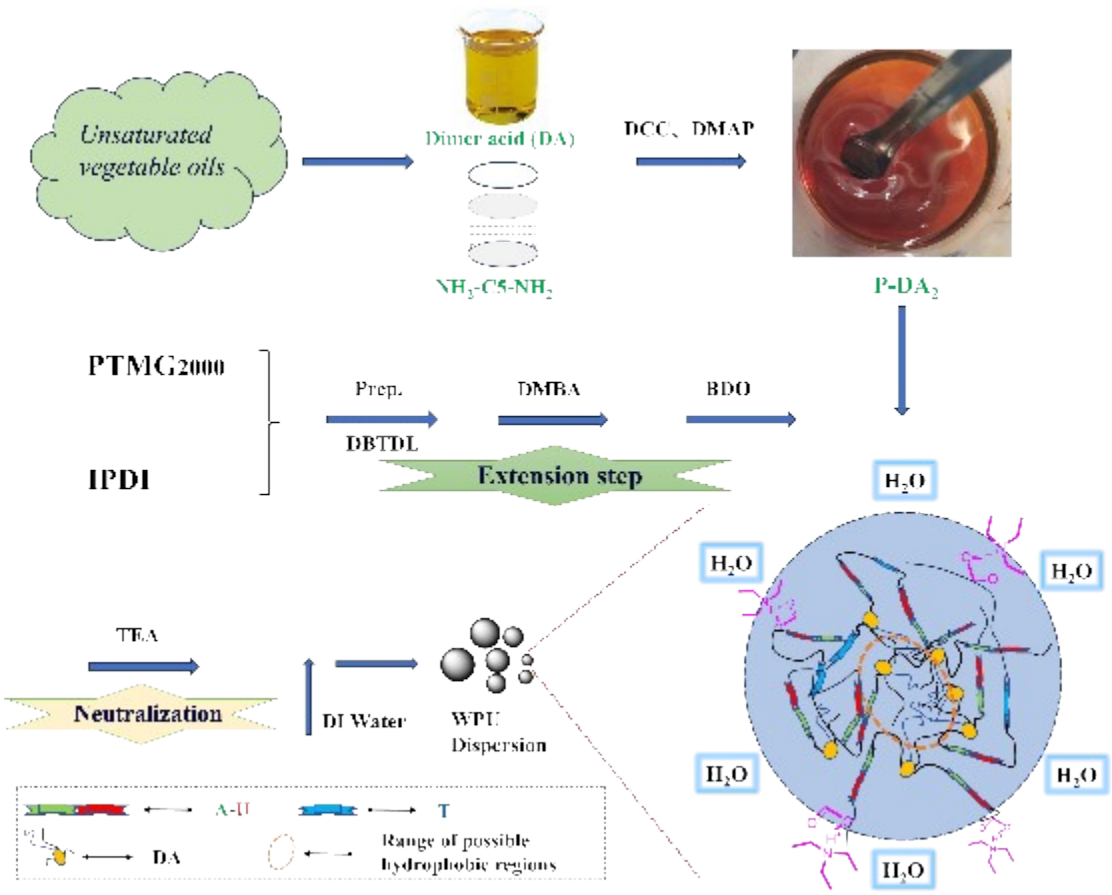

Fig. S7: Preparation process of W-P-DA_2-*x*% dispersion.

3 W-P-DA2-x% dispersion

Tab.S4 Characterization on W-P-DA_2-x% dispersion.

	Dispersion State					
P-DA_2-*x*%	Diameter (nm)	PDI	ζ Potential (mV)	Storage stability (month)	*η* (mPa·s)	Appearance
0	48.6	0.192	-37.3	>6	3	Blue Translucent
1	50.7	0.214	-38.0	>6	5	Slightly Yellow Translucent
2	51.9	0.205	-37.5	>6	5	Yellow Translucent
3	68.3	0.249	-38.1	>6	6	Yellow Translucent
4	64.9	0.274	-41.9	>6	5	Yellow Opaque
5	60.7	0.258	-41.2	>6	5	Yellow Opaque

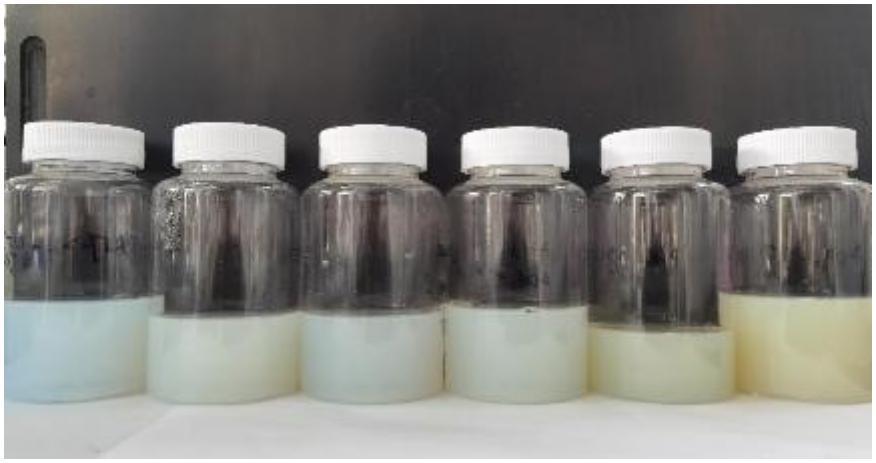

Fig.S8 W-P-DA_2-*x*% dispersion（W-P-DA_2-0%→5%, from the left to the right）

4 Characterization of W-P-DA$_2$-x% films

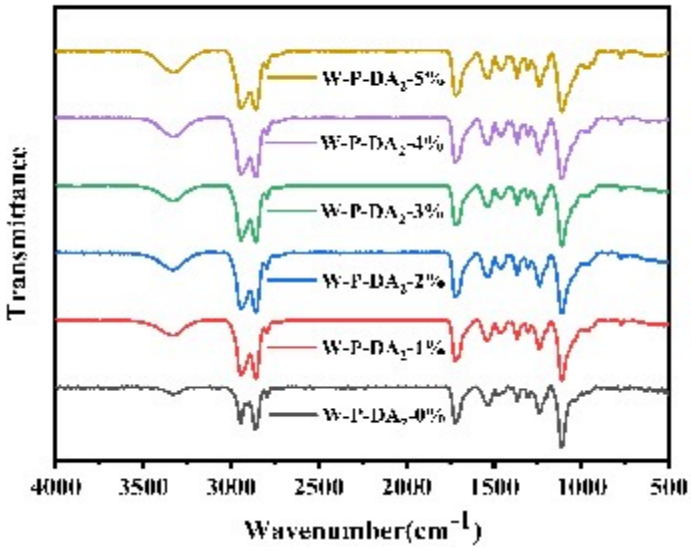

Fig.S9 FTIR of P-DA$_2$-x% WPU films.

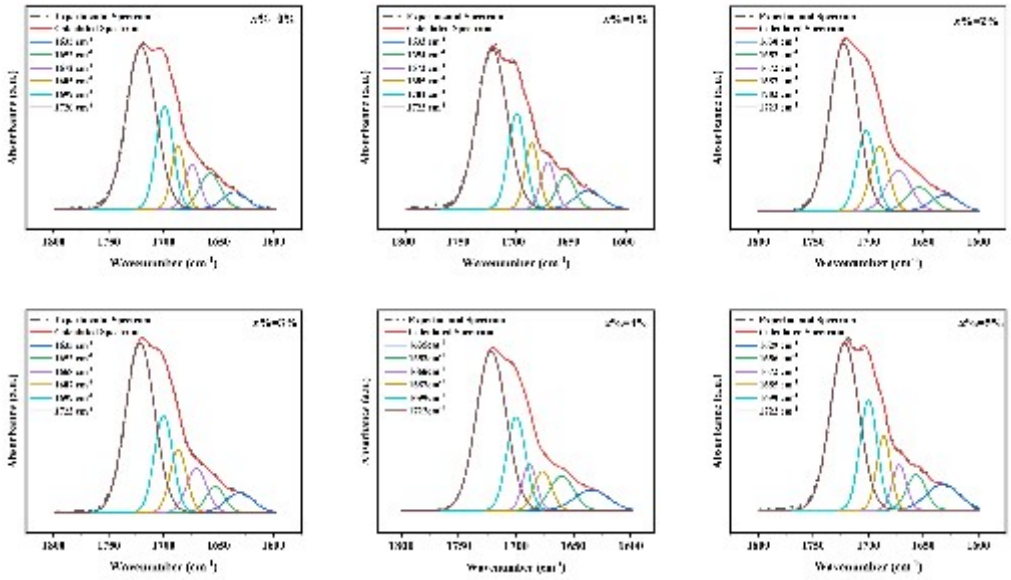

Fig.S10 The peak splitting and Gaussian fitting of the carbonyl (C=O) band

According to the integrated area percentage of the six bands in the fitted curves, the contribution(*C*%) of the different bonded and free carbonyl groups can be calculated as :

$$C\% = \frac{A_n}{A_1 + A_2 + A_3 + A_4 + A_5 + A_6} \times 100\% \text{.....} \quad \text{(Eq.S2)}$$

where in, A_n represents the fitted peak area, and n=1, 2, 3, 4, 5, 6 represent the peak areas of free(1722cm^{-1}), disordered(1699cm^{-1}, 1687cm^{-1}), and ordered(1667cm^{-1}, 1652cm^{-1}, 1635cm^{-1}) hydrogen bonding, respectively.

Tab.S5 Contribution percentages of individual C=O peaks from Gaussian fitting results.

x%	*C*（%）					
	1635 cm^{-1}	1652 cm^{-1}	1667 cm^{-1}	1687 cm^{-1}	1699 cm^{-1}	1722 cm^{-1}
0	3.87	7.41	7.08	9.22	19.19	53.23
1	5.39	6.66	7.20	9.92	17.79	53.05
2	5.53	6.48	10.25	12.89	12.89	51.96
3	7.34	8.73	6.97	7.25	18.99	50.73
4	7.61	6.86	9.87	6.56	21.18	47.92
5	8.46	6.85	10.50	10.52	19.43	44.23

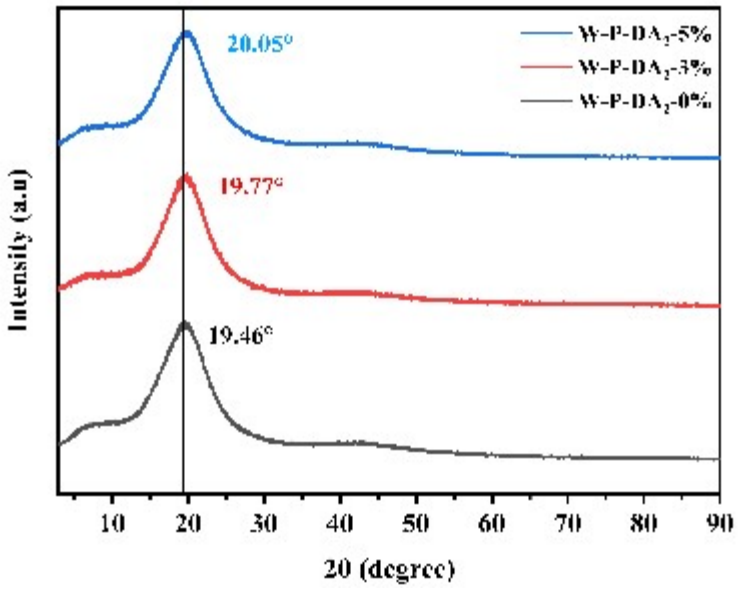

Fig.S11 XRD spectra of W-P-DA$_2$-0%, 3%, 5%.

Tab.S6 DMA characterization results of W-P-DA_2-*x*% films.

W-P-DA_2-*x*%	*E'* (MPa)	$T_{g,s}$(°C)	$T_{g,h}$(°C)	ΔT_g(°C)	E_a (kJ/mol)
0	2920	-59.8	90.4	150.2	33.8
1	2880	-58.2	76.6	134.8	\
2	2861	-54.5	62.6	117.1	\
3	3264	-54.6	60.3	114.9	\
4	3006	-54.0	73.1	127.1	25.9
5	2940	-52.2	86.7	138.9	\

5 Mechanical properties and water resistance

To calculate the fracture toughness, a notched specimen was used. The fracture energy (*Γ*) is calculated according to the following formula (Eq.S3).

$$\Gamma = \frac{6Wc}{\sqrt{\varepsilon_c}} \quad \text{.....(Eq.S3)}$$

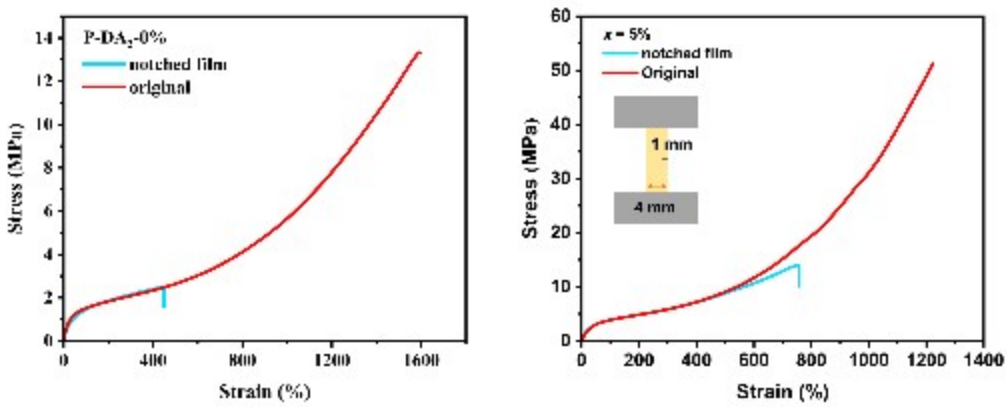

Fig.S12 Tensile curves of notched W-P-DA_2-x% samples.

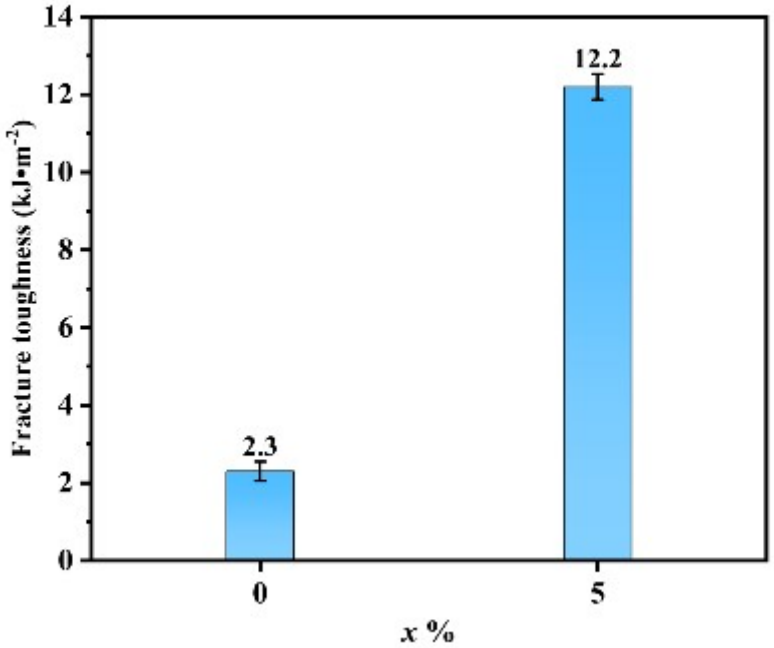

Fig.S13 Histogram of film fracture toughness calculated from Fig.S12.

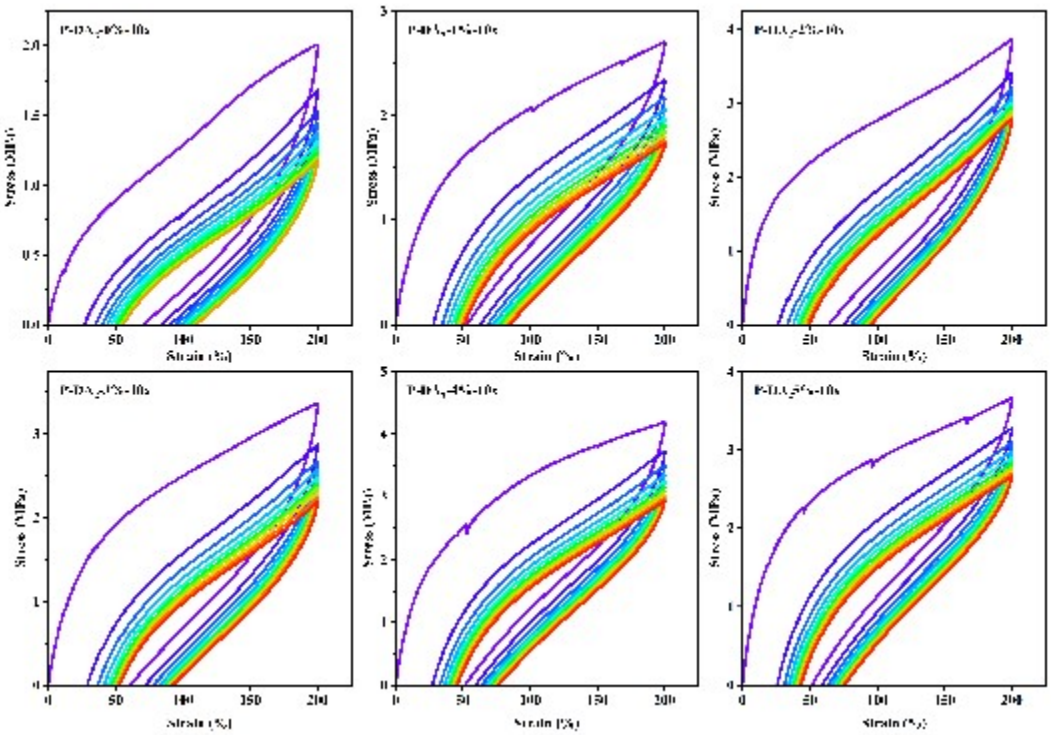

Fig.S14 Loading-unloading curves for 10 tensile cycles at 200% strain.

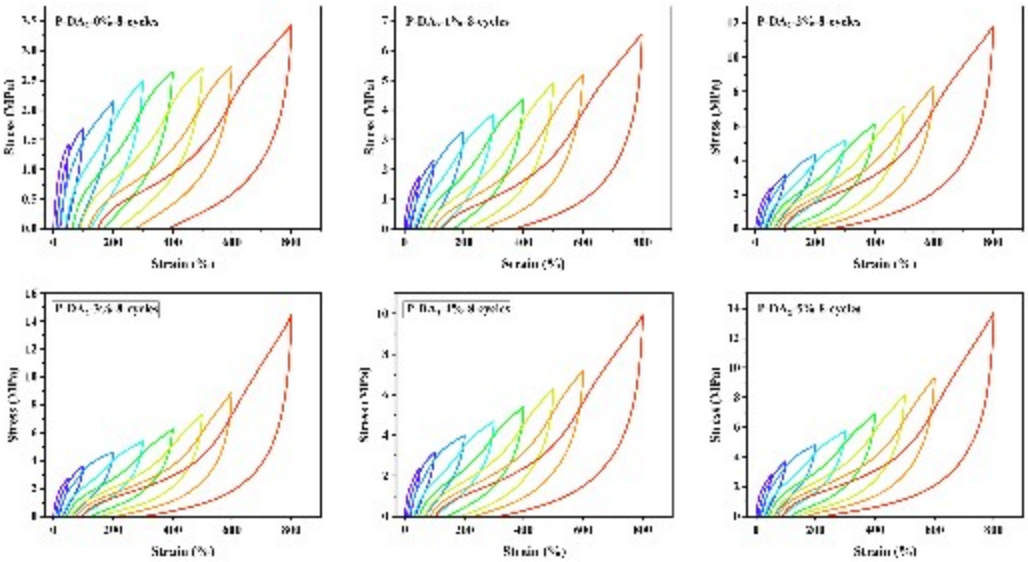

Fig.S15 Loading-unloading curves for varied strains.

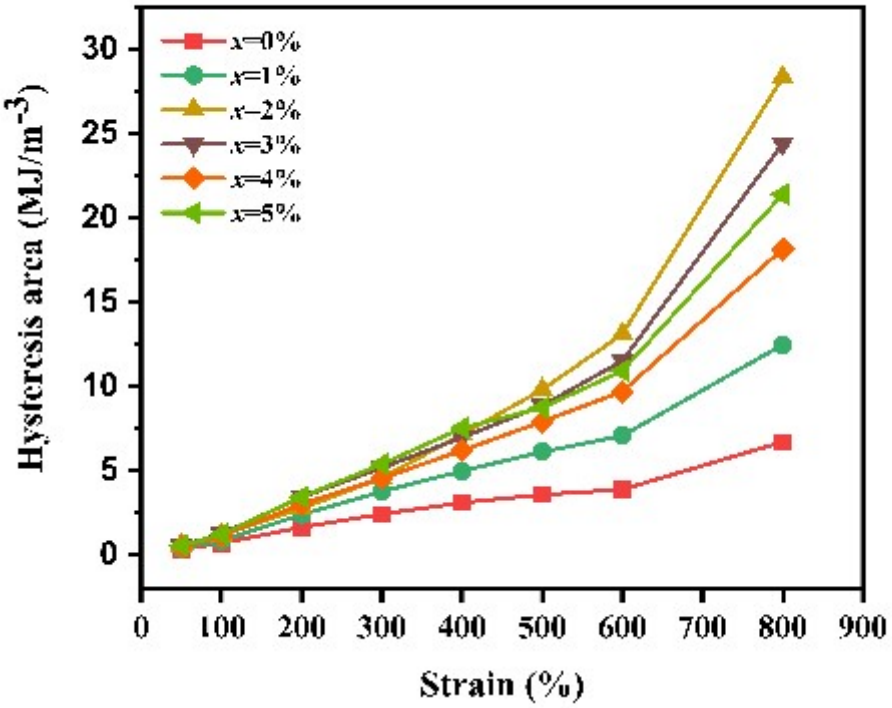

Fig.S16 The dissipated energy calculated from the hysteresis areas of the loading-unloading loops.

Fig.S17 Photograph of W-P-DA_2-4% films before, under and after weight loading.

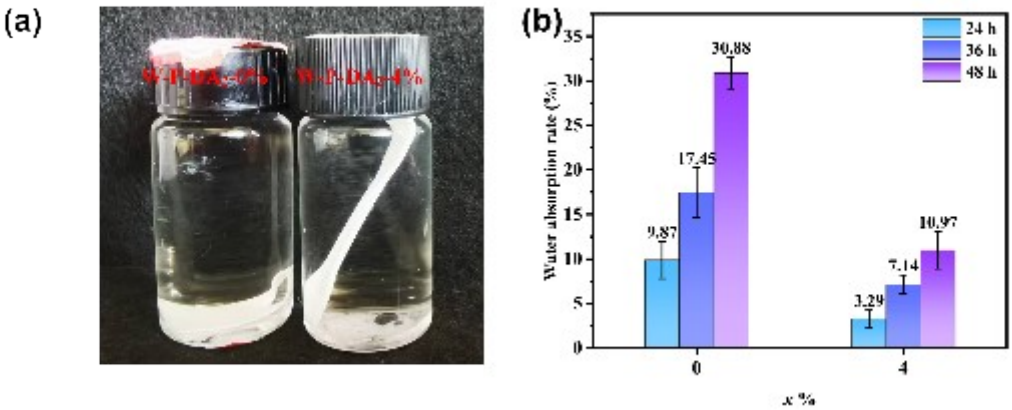

Fig.S18 (a) The films after 48 h of immersion in water; (b) water absorption rate at different immersion time.

Fig.S19 State of W-P-DA_2-*x*% films after immersion in water for 24 h (W-P-DA_2-0%→5%, from the left to the right).

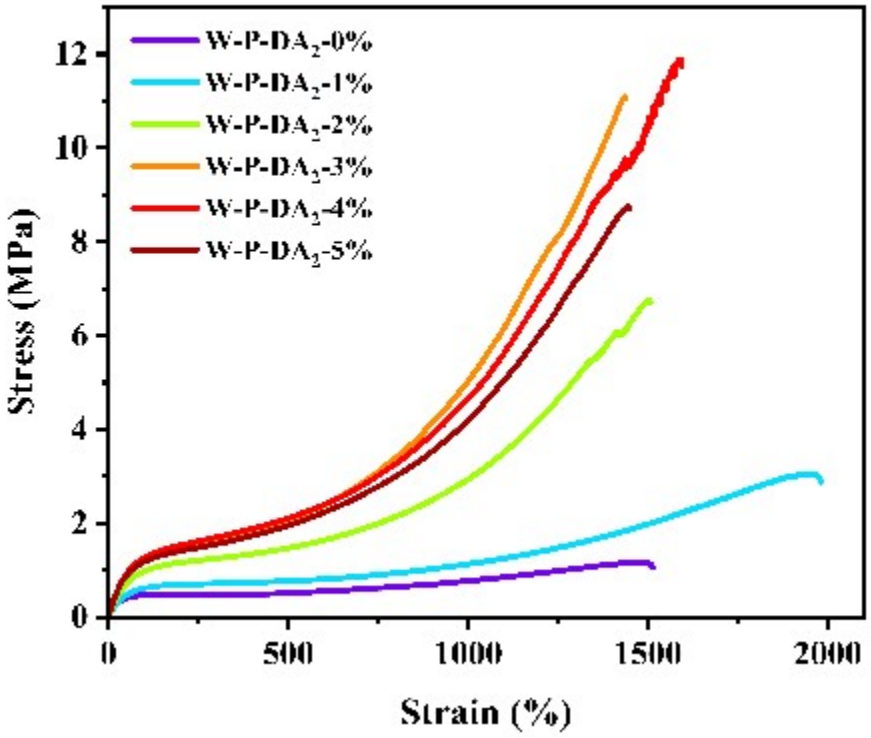

Fig.S20 Stress-strain curves of W-P-DA_2-*x*% film after 24 h of immersion in water.

6 Thermo-responsive self-healing

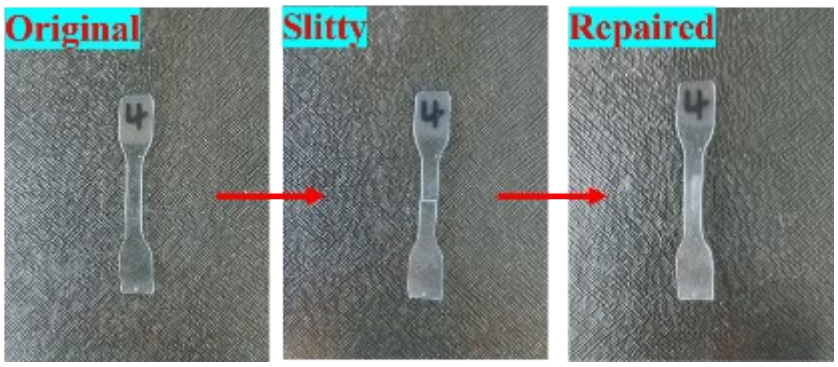

Fig.S21 The photographs of W-P-DA_2-4% before and after the self-healing.

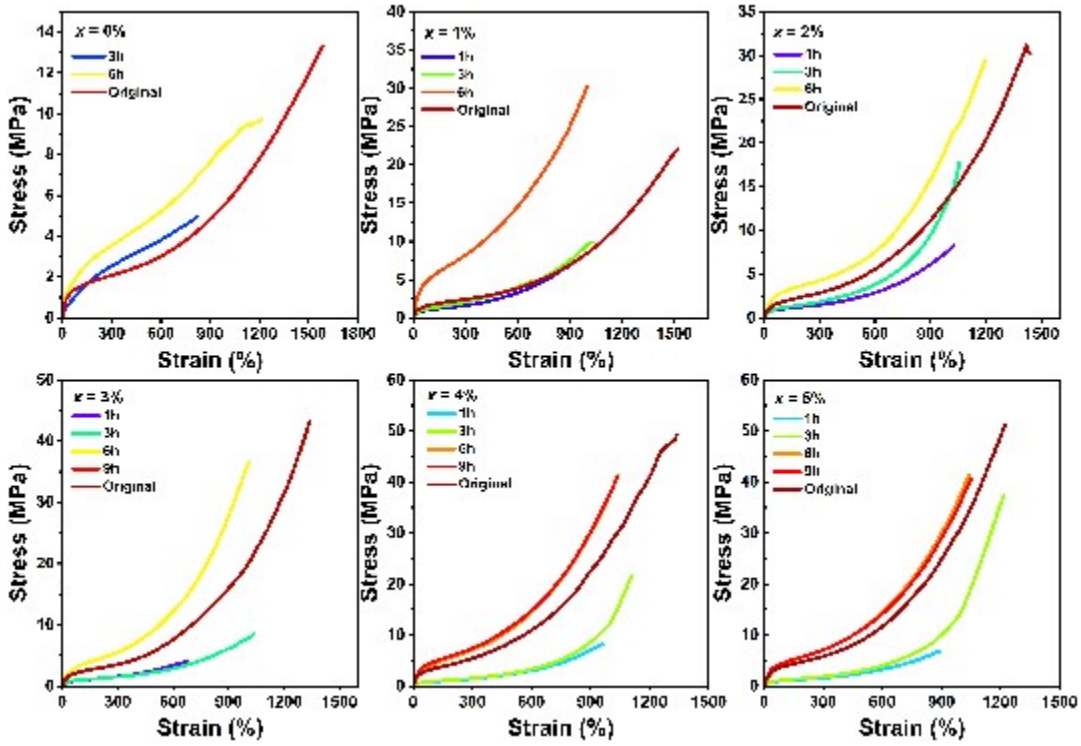

Fig.S22 Tensile curves of W-P-DA_2-*x*% films self-healing at 90°C for different time.

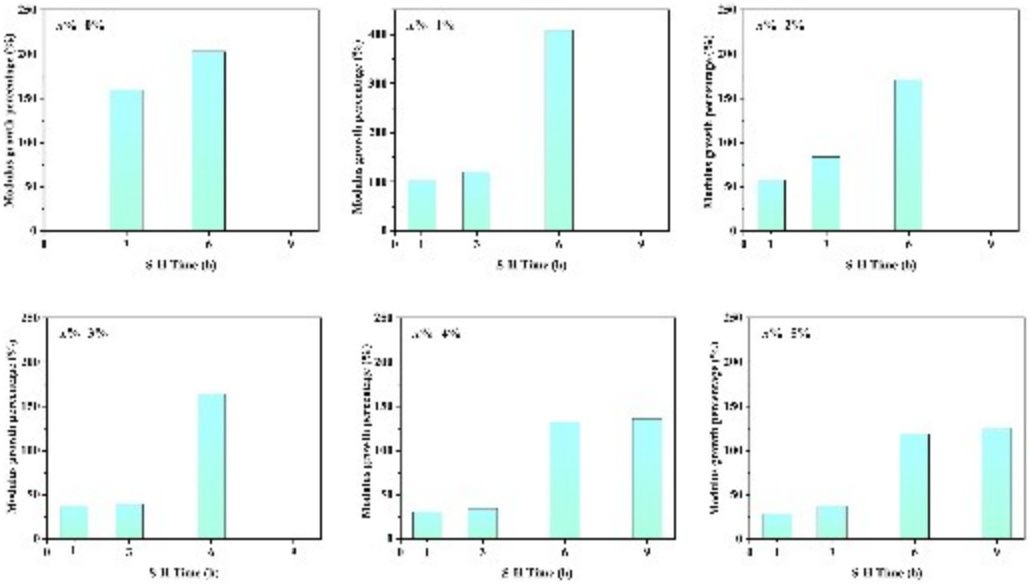

Fig.S23 Modulus growth percentage at 800% strain with the self-healing (S-H) time prolongation.

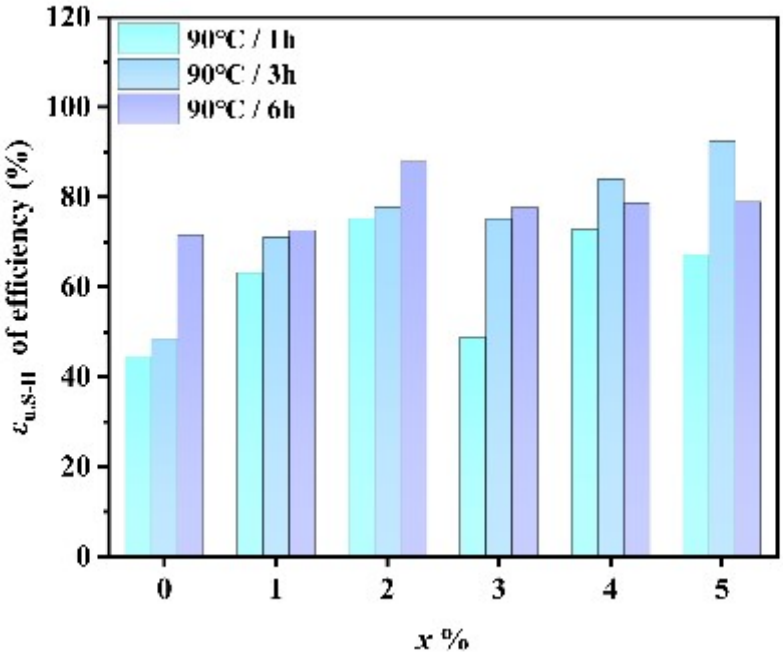

Fig.S24 Histogram of ε_u self-healing efficiency for different *x*% films as a function of self-healing time

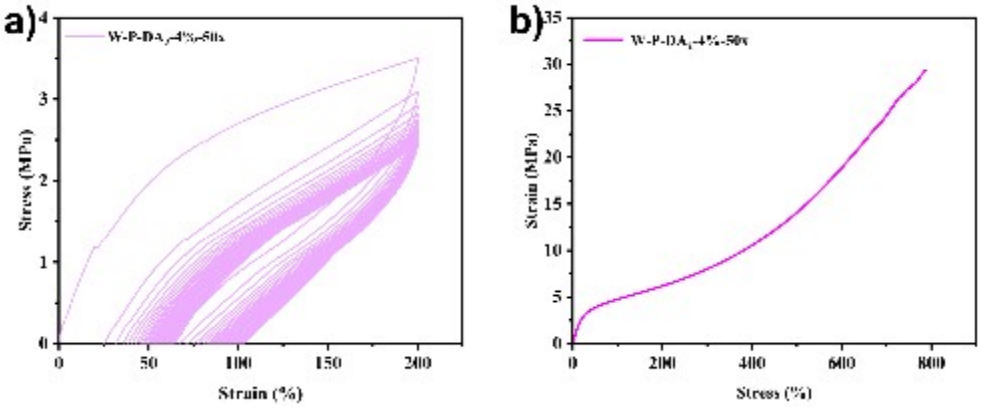

Fig.S25 (a) Loading-unloading cyclic tensile curves of W-P-DA_2-4% film after self-healing; (b) stress-strain curves of the spline used for loading-unloading cyclic tensile after self-repair.

Tab.S7 Comparative Summary of Literature Data.

	Tensile Strength/MPa	Self-healing elongation at break/%	Self-healing tensile strength/MPa
Ref 52	7.26	810	6.38
Ref 53	25	800	23
Ref 54	30.6	680	28
Ref 55	18	340	12
Ref 56	18.5	820	17.02
Ref 57	35.6	800	32.39
Ref 58	17.12	450.9	3.26
Ref 59	43.7	434	35.5
Ref 60	12	620	9.4
Ref 61	14.8	1090	13.8
Ref 62	21.8	1250	21.8
Ref 63	17.7	1300	12.56
Ref 64	16.9	1400	11.83
Ref 65	25.5	1800	24.73
Ref 66	18.7	2000	17.57
x% = 4%*	49.2	1039.6	41.1

* This work

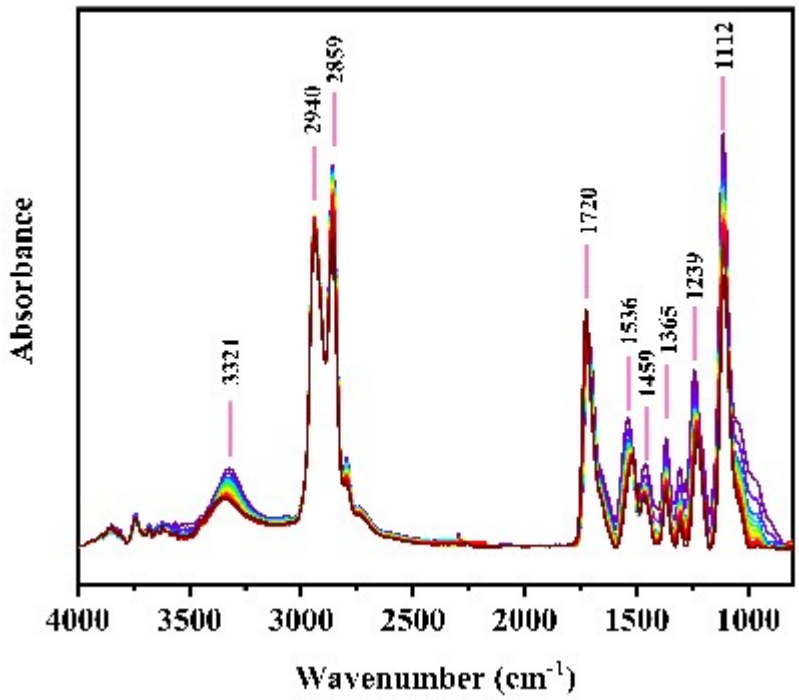

Fig.S26 Variable temperature infrared spectra of W-P-DA2-4% film at 40~150℃.

Tab.8 Summarized information on the cross-peaks of synchronous and asynchronous

Peak position (cm^{-1})	Synchronous	Asynchronous	Sequential order
1698, 1735	−	+	1735>1698
1630, 1735	−	+	1735>1630
1698, 1630	+	−	1630>1698

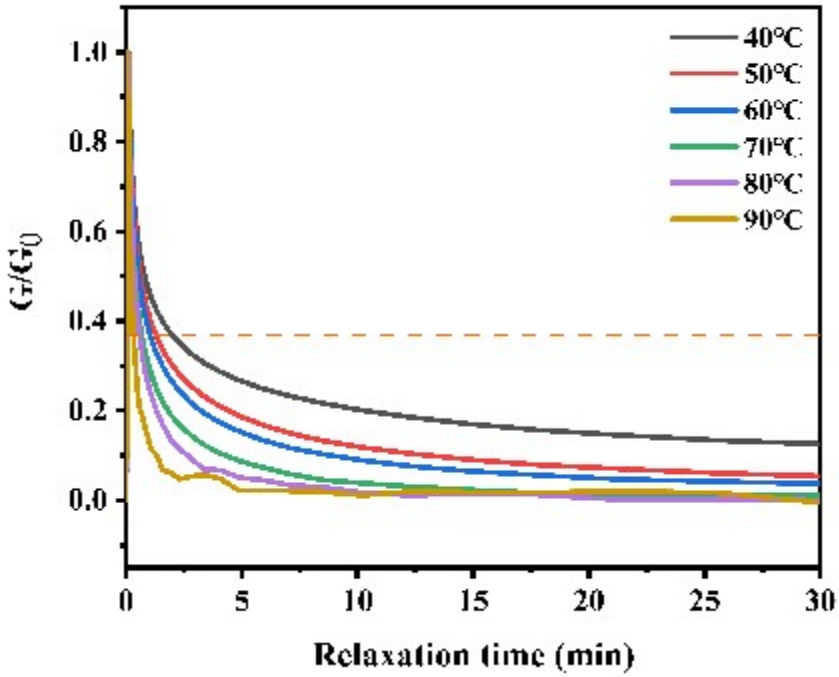

Fig.S27 Stress relaxation behavior of W-P-DA_2-0% film at different temperatures

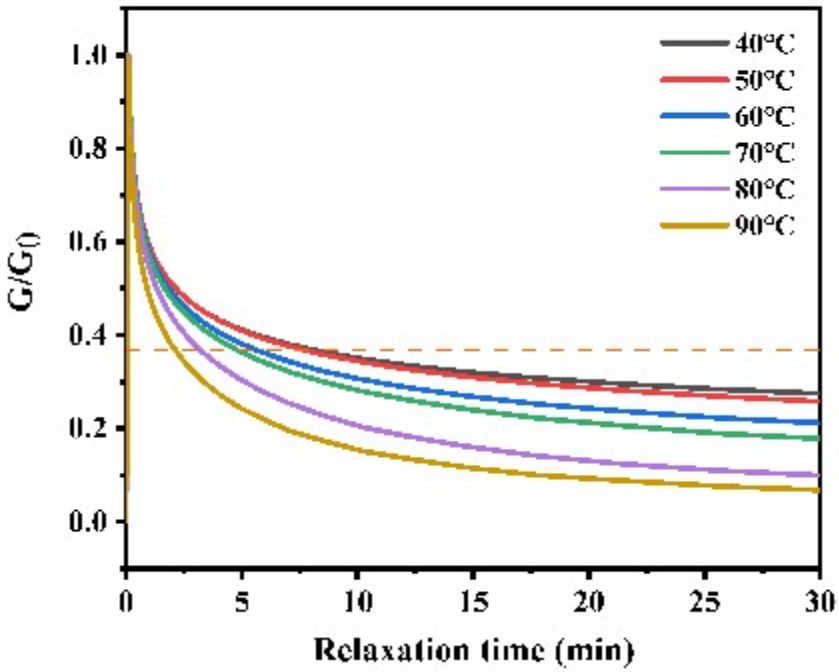

Fig.S28 Stress relaxation behavior of W-P-DA_2-4% film at different temperatures.

Calculation of activation energy (*Ea*) under stress relaxation for polyurethane films:

Using the Maxwell model, the time when G/G_0 of the polymer elastomer in the stress relaxation test decreases to $1/e$ is defined as the relaxation time (τ). The relationship between τ and temperature satisfies the Arrhenius equation, which is expressed as follows:

$$\tau = \tau_0 \, e^{\frac{\Delta E}{RT}} \tag{Eq.S4}$$

This equation can be simplified as:

$$ln\tau = ln\tau_0 + \frac{\Delta E}{RT} \tag{Eq.S5}$$

Where τ_0 represents the terminal relaxation time, which is the characteristic relaxation time at infinite temperature, T is the Kelvin temperature (K), ΔE is the activation energy for bond exchange, and R is the ideal gas constant (8.314 J/(mol·K^{-1})).

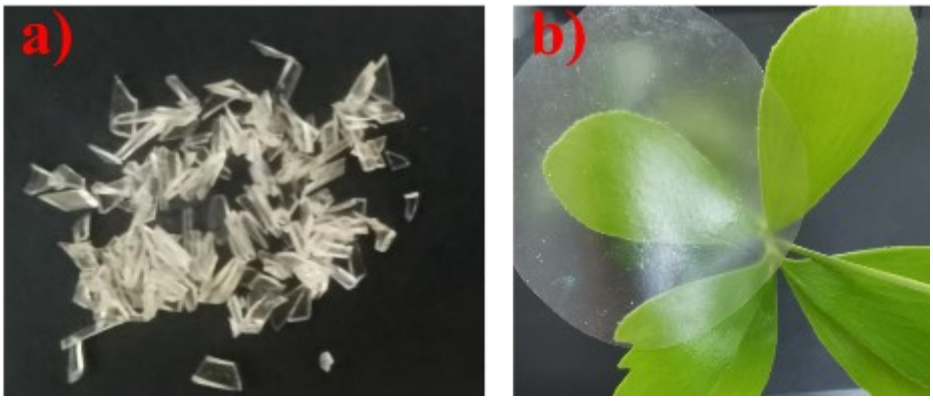

Fig.S29 Photograph of fragments of W-P-DA_2-4% film and its recovery.

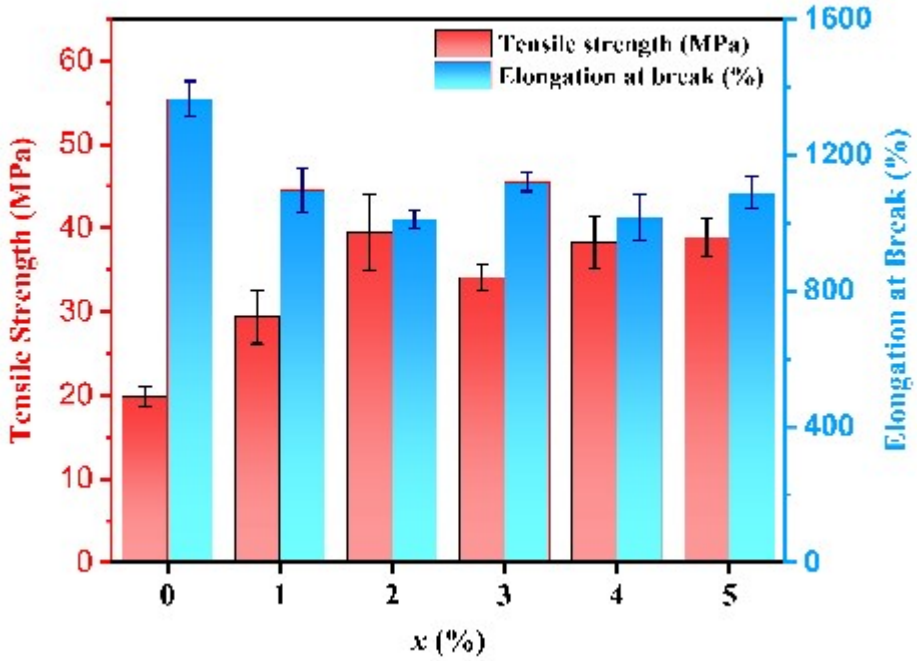

Fig.S30 Tensile strength and elongation at break of W-P-DA_2-*x*% film recovered from fragments after hot press processing at 120°C for 2 minutes.

7 Adhesion and strain sensitivity

Tab S9. Adhesion Strength of W-P-DA2-x% on Different Substrates.

Types of Adhesive Substrates	Adhesive Strength of W-P-DA_2-x% Dispersion (MPa)					
	0%	1%	2%	3%	4%	5%
PPTA	3.10	3.76	3.77	4.34	3.88	3.38
NBR	3.09	4.16	5.10	5.31	5.75	4.52
NR	0.51	0.53	0.55	0.56	0.58	0.58
Wood-original (1st)	0.46	0.48	0.49	0.72	1.50	0.85
Wood-2nd	1.05	1.08	1.67	2.25	2.73	2.60
Wood-3rd	1.45	1.83	2.29	2.49	3.99	2.76
Al Sheet	3.02	3.21	3.24	3.43	2.87	2.84
Cu Sheet	0.27	0.58	0.72	0.84	0.91	1.05
PE Sheet	0.20	0.23	0.23	0.31	0.28	0.29

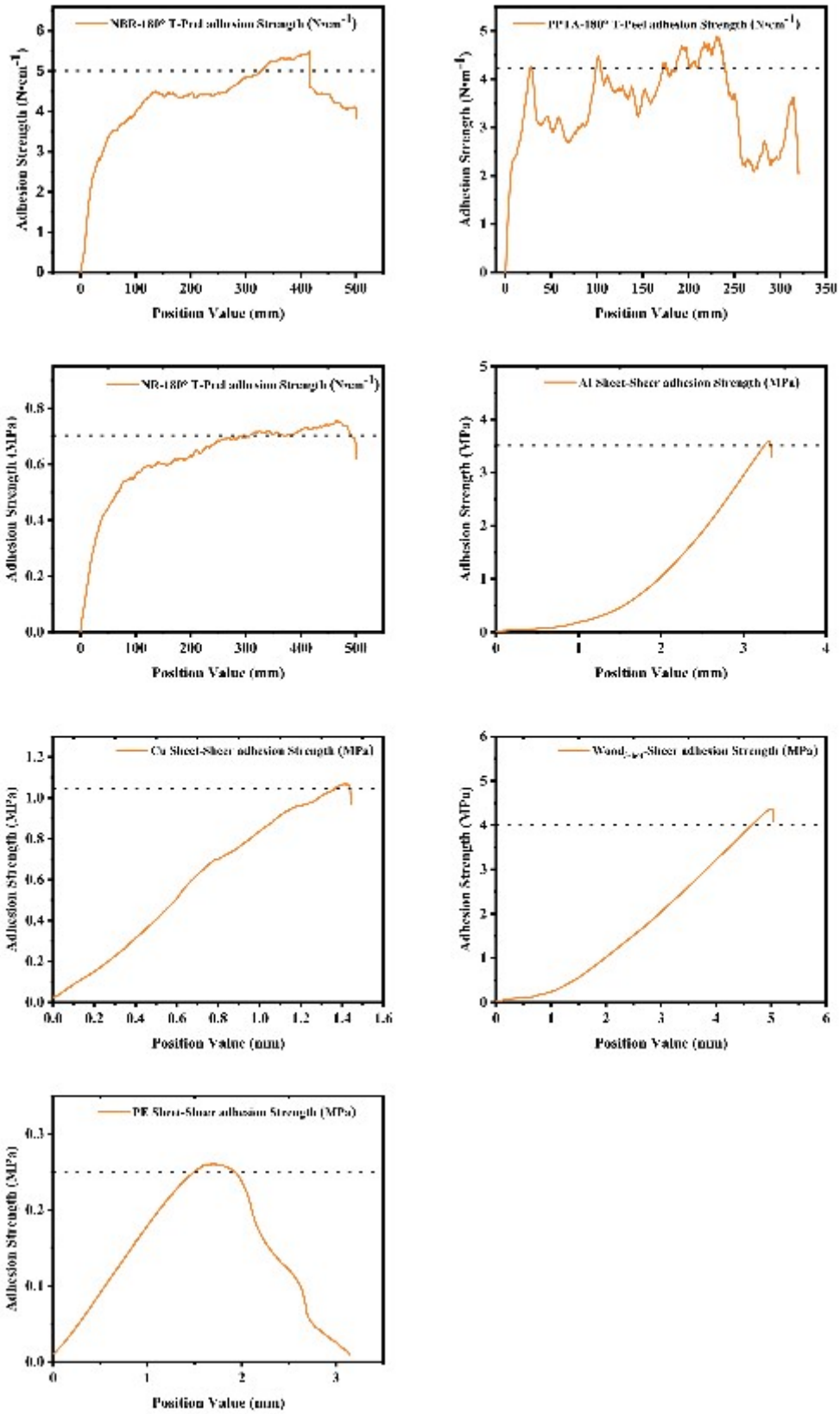

Fig.S31 Adhesion strength test curves of W-P-DA_2-*x*% bonded samples.

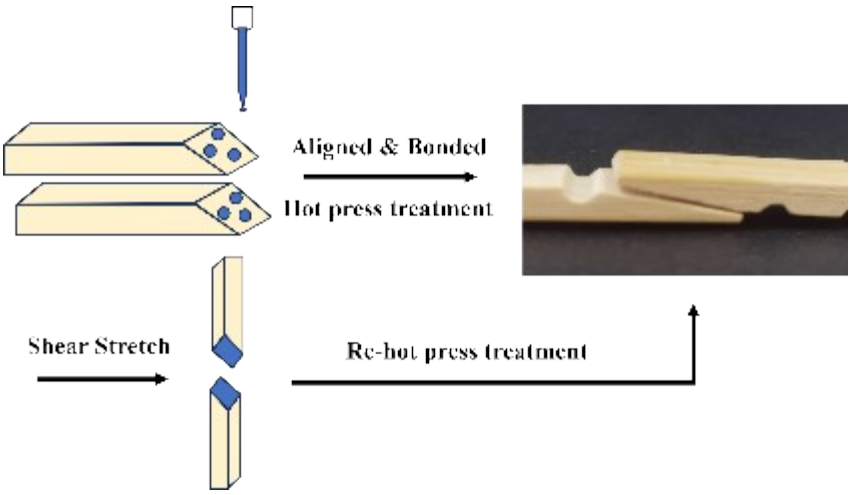

Fig.S32 Wood bonding-destruction-rebonding cyclic process.

Tab.S10 Specific parameter changes for Li^{+}_{m}-W-P-DA_2-4%

C_{Li^+} (moL·L^{-1})	Salt precipitation effect	Resistance signal	σ(S·m^{-1})	Tensile strength(MPa)	Elongation at break(%)	Film adhesion
0.05	not	×	\	28.9	922	Not
0.10	not	√	1.10×10^{-9}	9.77	1387	Not
0.15	not	√	2.30×10^{-9}	2.16	1354	Not
0.20	Flocculent	√	3.42×10^{-5}	1.50	2527	Weak
0.30	Saline gel	√	3.58×10^{-4}	1.73	1598	Little strong
0.40	Saline gel	√	7.09×10^{-4}	1.73	1366	Strong
0.50	Saline gel	√	1.20×10^{-3}	1.37	1252	Strong

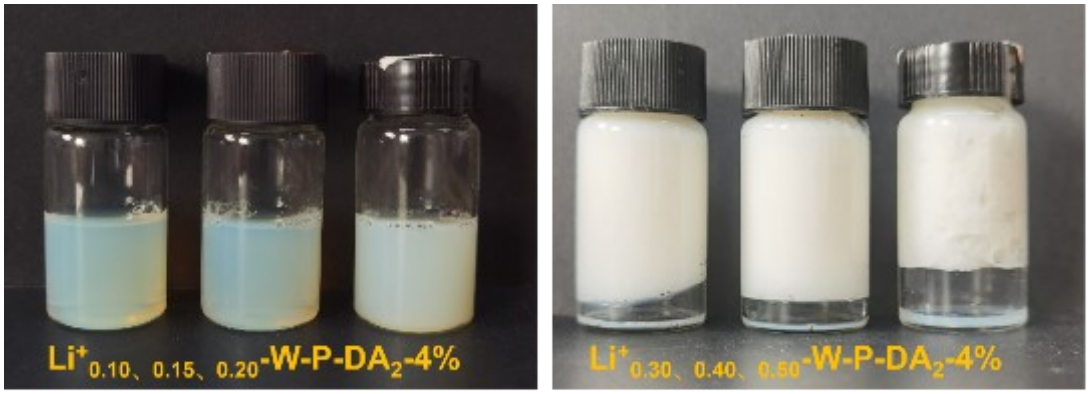

Fig.S33 Salt precipitation effect of Li^{+}_{m}-W-P-DA_2-4%

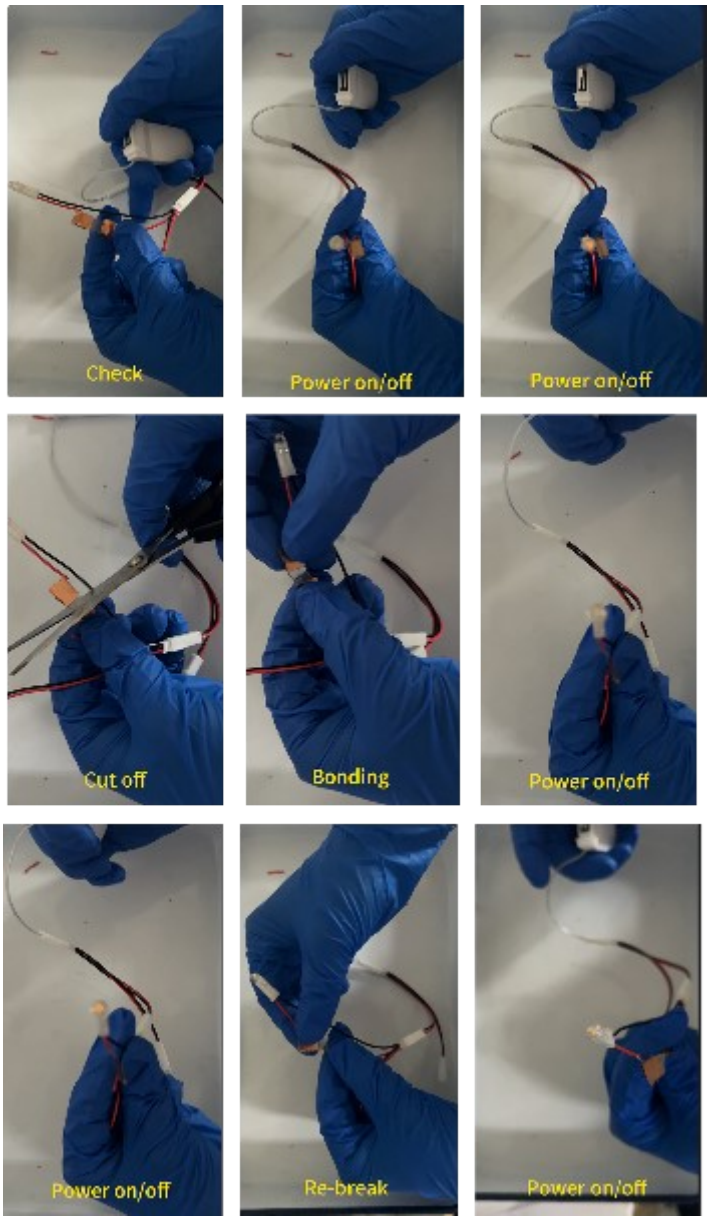

Fig.S34 Changes in LED lights under various states of $Li^{+}_{0.4}$-W-P-DA_2-4% composite film.

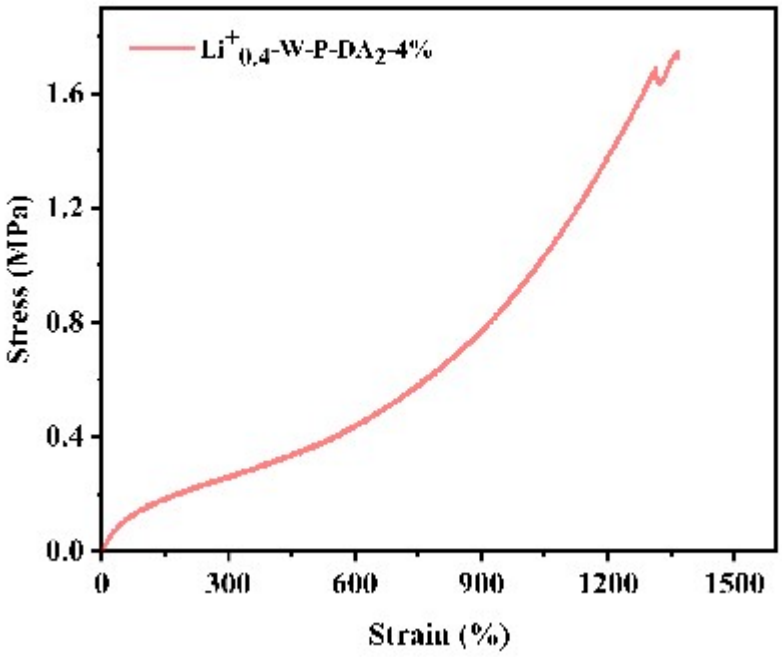

Fig.S35 Tensile curve of $Li^{+}_{0.4}$-W-P-DA_2-4% composite film.

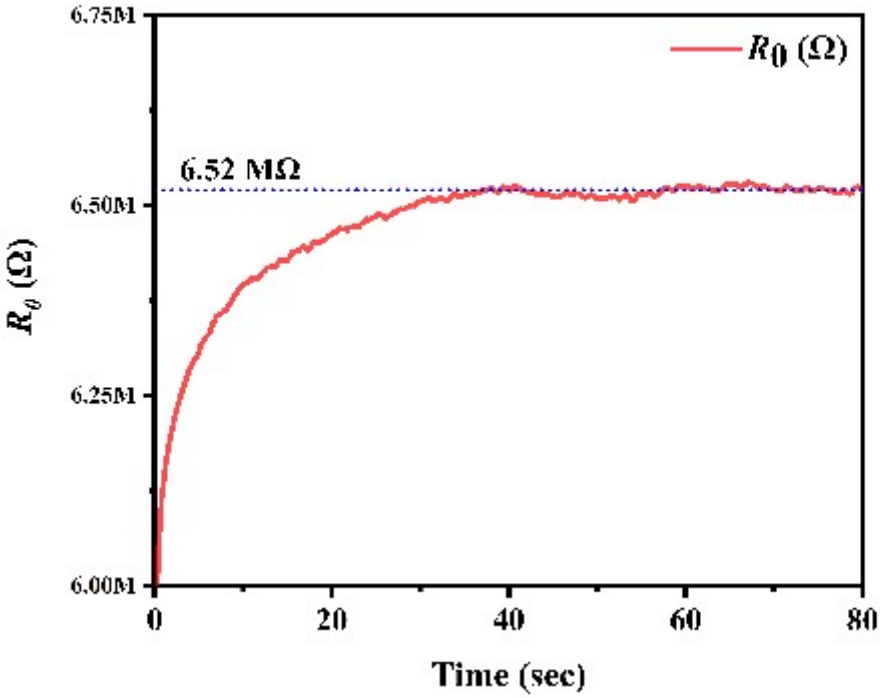

Fig.S36 Time related resistance varision of $Li^{+}_{0.4}$-W-P-DA_2-4% film.

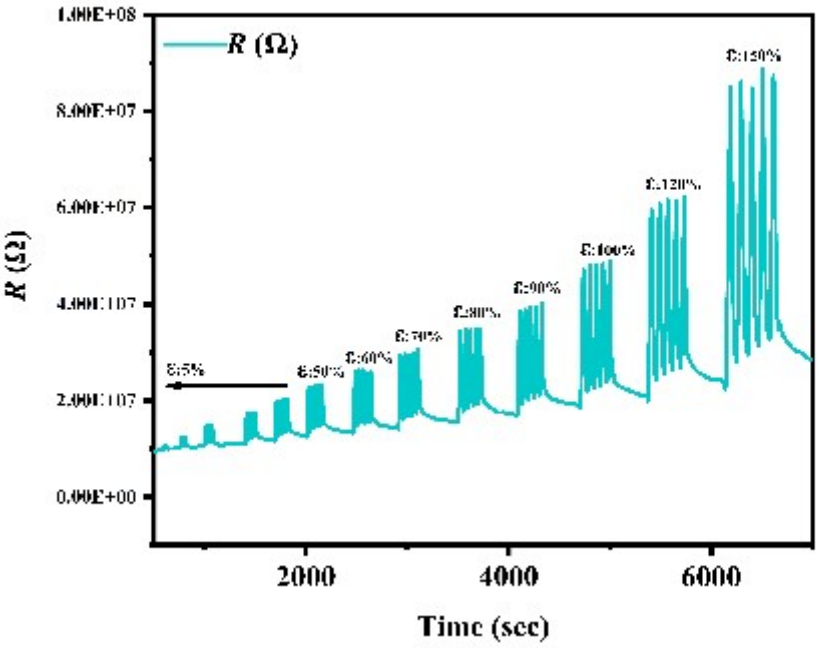

Fig.S37 Time related resistance varision under different strains.